ENGINEERING RESEARCH JOURNAL (ERJ)

Vol. 1, No. 49 Jul. 2021, pp 122-144

Journal Homepage: http://erj.bu.edu.eg

Web crippling strength of Cold Formed Steel Z-Sections Subjected to Interior One Flange Loading.

Mohamed Saied Refaee Saleh[1], Mohamed Salah Soliman[1], Fathy Abdelmoniem Abdelfattah[1] and Anwar Badawy Badawy Abu-Sena[1]

1 - Faculty of Engineering (Shoubra), Benha University, Egypt.

Abstract This paper presents an experimental and numerical investigation into web crippling resistance of unfastened cold formed steel Z-sections subjected to Interior One Flange (IOF). Both Z-sections have stiffened and unstiffened flanges were studied. This paper presented the results of 12 test specimens considering the IOF loading condition. A verified finite element models were developed to simulate the experimental tests. An extended parametric study was carried out based on the verified finite element models. The parametric study included the different factors affecting the web crippling resistance such as; material yield stress, web thickness, inside bend radius, web depth and bearing load length to thickness ratios. The web crippling strength according to the Eurocode EN 1993-1-3 and the North American specification AISI S100-16 were compared to the experimental and the finite element results. The comparisons showed that the two specs; Eurocode EN 1993-1-3 and AISI S100-16 overestimated the web crippling strength of the studied range of cold formed steel Z-sections. Modifications were proposed to improve the design standard predicted resistances.

Key words: Web crippling, Cold formed steel, Z section, Interior one flange loading, and Finite element analysis

Nomenclature	
b	Flange width
C, C_N, C_R & C_h	Web crippling coefficients
D	Web depth
ds	Lip depth
E	Young's modulus of steel, = 210 kN/mm^2
F_u	Ultimate stress
F_y	Yield stress
h	Flat web height
h_w	Web height measured between mid-flanges thickness
k, k_1, k_2, k_3, k_4 & k_5	Web crippling coefficients
L	Specimen length = $N+2D+200$ mm
N	Load bearing length
P	Applied load, kN

P_n	Nominal web crippling strength
R	Inside bend radius
R_{wd}	Web crippling resistance
t	Web thickness
ux	Lateral web deformation
uy	Vertical web depression
εu	Total elongation

1. Introduction

Cold formed steel sections are generally fabricated from light gauge steel sheets by rolling or press break methods. In practice, the most common cold formed steel sections are C and Z sections. These sections are used as secondary members in steel construction due to their high strength to weight ratio. In beams of such sections, it is not common to use stiffeners under concentrated loads so that, the web crippling is one of the main failure modes. The web crippling is local failure occurs in form of web buckling under concentrated loads.

Numerous researchers investigated the web crippling of cold formed steel sections experimentally and found that; the Web crippling load is a function of many factors such as; material yield stress, cross section geometry, applied load pattern, loaded length and the flange restraining condition. Most of these researches were conducted on cold formed steel C-sections and little on Z-sections. Here after; brief of literature survey on researches concerned with cold formed steel C and Z-sections.

Bhakta et al. [1] investigated the effect of fastened flanges on the web crippling of C and Z-sections subjected to End One Flange (EOF) loading condition. It was observed that, the fastened flanges in case of Z-sections increased the web crippling load by 30% while in case of C-sections the increase was 3%.

Cain et al. [2] carried out a similar investigation for web crippling of Z-sections subjected to EOF loading condition. The results showed an increase in the web crippling load by 41%. The predicted web crippling strengths by the American specification (AISI-1986) [3] showed underestimation for fastened flange specimens when compared to the test results.

Gerges and Schuster [4] investigated the effect of large inside bend radius on the web crippling strength of C-section subjected to EOF loading. The test specimens had the same web thickness and the yield stress. The test specimens were varied in; the overall web depths (D), the bearing plate length (N) and the inside bend radius (R). The test results were compared to the American specification (AISI-1996) [5] and the Canadian standard (CSA S136-94) [6]. The design specification showed underestimation for the predicted web crippling strength against the test results.

Beshara and Schuster [7] investigated the effect of increasing the overhanging length on the web crippling strength of C and Z-sections under Interior Two Flange (ITF) and End Two Flange (ETF) loading conditions. The specimens were fabricated so that; the specimen lengths were more than five times the depth, the inside bend to thickness R/t ratios were up to 12 and the flanges were fastened to the support. Comparisons of the test results showed that, Z-sections experienced a higher web crippling load than C-sections by 20% in case of ETF loading and (10 to 20)% in case of ITF loading. The test results experienced an increase of 50% and 5% for ITF and ETF loading when compared to the predicted strengths by AISI-1996 [5].

Young and Hancock [9-10] investigated the web crippling of C-sections having unfastened lipped and un-lipped flanges under four loading

conditions (EOF, IOF, ETF and ITF). The test specimens were unfastened to supports and had web height to thickness ratios *h/t* ranged from 15 to 45. The test loads were compared to the predicted strengths by AISI-1996 [5] and the NAS-2001 [8] specifications. The comparisons showed that, the AISI-1996 [5] overestimated the web crippling strength of C-sections having un-lipped flanges and conservatively estimated the web crippling of C-sections having lipped flanges. On the other hand, predicted web crippling strength by the NAS-2001 [8] was conservative for C-sections under ETF and ITF and un-conservative for C-sections under EOF and IOF loading conditions. Young and Hancock [11] investigated experimentally the effect of flange restraints on the web crippling strength of C-sections subjected to ETF and ITF loading conditions. The test results were compared to the predicted strengths using the NAS-2001 [8]. The comparisons showed that, the NAS-2001 [8] was conservative for C-sections with unfastened flanges and un-conservative for C-sections having fastened flanges.

Holesapple and LaBoube [12] investigated the effect of the overhanging length beyond the end support on the web crippling strength of C and Z-sections subjected to EOF loading conditions. The test results were compared to the NAS-2001 [8] which found conservative in predicting the crippling load for overhanging length less than 1.5*h* and un-conservative for more than 1.5h if IOF was considered. A modification factor was proposed for the case of overhanging length beyond the EOF loading conditions.

Macdonald et al. [13-14] carried out experimental tests on the web crippling of C-sections having lipped flanges under the four loading conditions; EOF, IOF, ETF and ITF. Macdonald et al. [13-14] developed nonlinear finite element models for simulating the web crippling failure of the tests. The results from tests and finite element analysis were compared to the web crippling strengths predicted The Eurocode 3, Part 1.3 [15]. The comparisons showed that, the Eurocode3 underestimated the web crippling of the test specimens under ETF and EOF loading conditions by 48% and 34% respectively. Based on the results from tests and nonlinear finite element analysis a parametric study was carried out and a design unified rule for the four loading conditions was developed. The parametric was based on; constant web thickness ($t = 0.78\ mm$) and yield stress ($F_y = 220\ N/mm^2$), varied corner radii ($R = 1.2, 2.6, 3, 4, 5\ mm$), varied web depth ($h = 50, 75, 100, 150\ mm$) and varied load bearing lengths ($N = 25, 50, 75, 100\ mm$).

Gunalan and Mahendran [16] investigated the web crippling of C-sections having un-lipped and stocky webs of thickness t ranged from 3.8 to 8.0 mm and subjected to ETF and ITF loading conditions. The specimens were unfastened to supports. The test results were compared to the web crippling strength from the Australian standard (AS/NZS 4600) [17] and the North American specification (AISI S100-2007) [18]. The comparisons showed that, the design standards; AS/NZS 4600 [17] and AISI S100-2007 [18] were un-conservative for stocky webs.

Sundararajah et al. [19-20] investigated the web crippling capacity of C-sections having lipped flanges and fabricated from high strength steel. The specimens were tested under the four loading conditions; EOF, IOF, ETF and ITF. The test results were compared to the predicted strengths from the American, Australian and European [21, 17and 15]. For EOF loading, the predicted design strengths from AISI S100-2012 [21] and AS/NZS 4600 [17] were un-conservative when compared to the test loads, while Eurocode 3, Part 1.3 [15] was overly conservative. For IOF loading, the comparisons showed that, Eurocode 3, Part 1.3 [15] was very conservative, whereas AISI S100-2012 [21] and AS/NZS 4600 [17] agreed well with the test loads.

Due to the above literature survey it was observed that, most of researches on web crippling of cold formed steel C and Z- sections are experimental and little of these researches which concerned with Z-sections. It was observed also that, almost no researches studied the web crippling of Z-sections under IOF loading. Accordingly, this study focused on investigating the web crippling for lipped and un-lipped Z sections shown in figure 1, subjected to IOF loading conditions. This study concerned with the un-fastened flanges to support locations. The study included experimental tests and verified nonlinear finite element models to study the influence of different parameters on the web crippling strength. The considered parameters were; web height (h) and thickness (t), inside bent radius (R), lip depth (ds) and load bearing length (N).

Two design standards were considered to estimate the web crippling strength of studied range of specimens and models; The North American specification AISI S100-16 [22] and the Euro code EN 1993-1-3 [15]. The results obtained from the

experimental tests and nonlinear finite element analysis were compared to the predicted web crippling strength from the considered design standards.

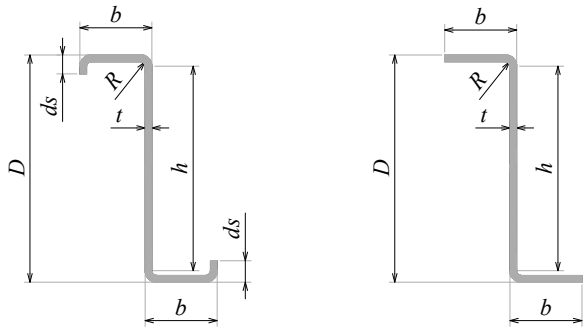

Figure 1: Definitions of Z-sections with lipped and un-lipped flanges.

2. Test Program

The test program was designed to study the effect of different cross section geometries such as *t*, *h* and *ds* and different values of loading lengths *N* on the web crippling strength of cold formed steel Z sections with un-fastened flanges at IOF loading condition.

2.1 Test Specimens

A total number of 12 cold formed steel Z –sections were tested in study for web crippling under IOF loading conditions. The specimens were fabricated by press brake method with constant inside bent radius (R =2 mm) due to the manufacturing capabilities. The cross section dimensions and lengths of the test specimens were listed in Table 1. The specimen labels were designated such that the cross section dimensions in Figure 1 could be recognized. For example, specimen label (*Z150×62×16×1.5-R2-N30)* defined the following; web depth *D = 150 mm*, flange width *b = 62* mm, lip depth *ds = 16 mm*, web thickness t = 1.5 mm, inside bent radius R = 2 mm and load bearing length *N = 30 mm*. The length of the test specimens *L* was calculated to satisfy the minimum requirements of the considered design standards; AISI S100-16 [22] and EN 1993-1-3 [15] for IOF loading condition. The minimum requirement to satisfy the IOF loading was to keep the distances between the edges of exterior and interior load bearing plates not less than 1.5 times the web depth *D* as shown in Figure 2. The lengths of exterior load bearing plates were kept constant value of 100 mm to force the failure occurs at mid span and under IOF loading conditions.

Table 1: Dimensions of test specimens.

Specimen		*D,* mm	*b,* mm	*ds*, mm	*t*, mm	*R,* mm	*N*, mm	*L*, mm
No.	Label							
S1	Z150×62×16×1.5-R2-N30	150	62	16	1.5	2.0	30	680
S2	Z202×60×00×0.9-R2-N30	202	60	0	0.9	2.0	30	830
S3	Z204×62×16×1.4-R2-N30	204	62	16	1.4	2.0	30	830
S4	Z204×64×16×1.9-R2-N30	204	64	16	1.9	2.0	30	830
S5	Z204×62×00×1.5-R2-N30	204	62	0	1.5	2.0	30	830
S6	Z204×62×16×1.4-R2-N50	204	62	16	1.4	2.0	50	850
S7	Z204×60×00×1.5-R2-N50	204	60	0	1.5	2.0	50	850
S8	Z204×62×16×1.4-R2-N100	204	62	16	1.4	2.0	100	900
S9	Z202×62×00×1.4-R2-N100	202	62	0	1.4	2.0	100	900
S10	Z254×62×16×1.5-R2-N30	254	62	16	1.5	2.0	30	980
S11	Z202×62×16×1.1-R2-N30	202	62	16	1.1	2.0	30	830

S12	Z203×62×16×1.0-R2-N100	203	62	16	1.0	2.0	100	900

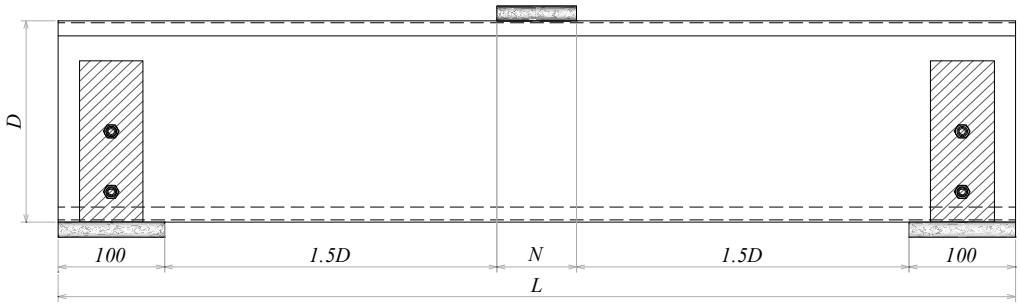

Figure 2: Test specimen arrangement

2.2 Material Properties

Three tensile tests were carried out to determine the material properties of the test specimens. Three test specimens with different thicknesses specimens were prepared according to ASTM A370 [23] to carry out the tensile tests. The tensile tests results were listed in Table 2; the yield stress (F_y), the ultimate stress (F_u) and the total elongation (εu).

Table 2: Material Properties of tests specimens

Specimen thickness *t,* mm	Yield Stress $F_{y,}$ N/mm^2	Ultimate Stress, $F_{u,}$ N/mm^2	Elongation εu %
1.0	298	373	25.1
1.5	345	414	28.0
1.9	398	457	22.1

2.3 Test Setup and Procedure

The universal testing machine Shimadzu of 500 kN loading capacity was used to carry out the web crippling tests in this research. A steel beam of built up I-section, with transverse stiffeners at equal distances was placed on the fixed part of the testing machine and considered the base on which the test specimens supported, Figure 3. The roller and hinge supports of the test specimens were installed on the built up steel beam. The end bearing plates of constant length 100 mm and thickness 20 mm were placed between the bottom flange of test specimens and the roller/hinge supports as in Figure 4. Wooden blocks were attached to the web of test specimens at support locations to prevent the rotation of test specimens and insure that no web crippling occurs at support locations. The use of wooden blocks was also adopted by Macdonald et al, [13, 14]. The testing load was gradually applied to the placed load bearing plate at mid span of the test specimen through the loading jaw. Two LVDTs were installed at mid span of test specimens to measure the lateral web displacement ux and vertical displacement uy of the bottom flange as shown in figure 4. The LVDTs and the loading cell of the testing machine were connected to multi-channels data logger which recorded the load, the displacements of LVDTs and the vertical movement of the loading jaw during the testing process.

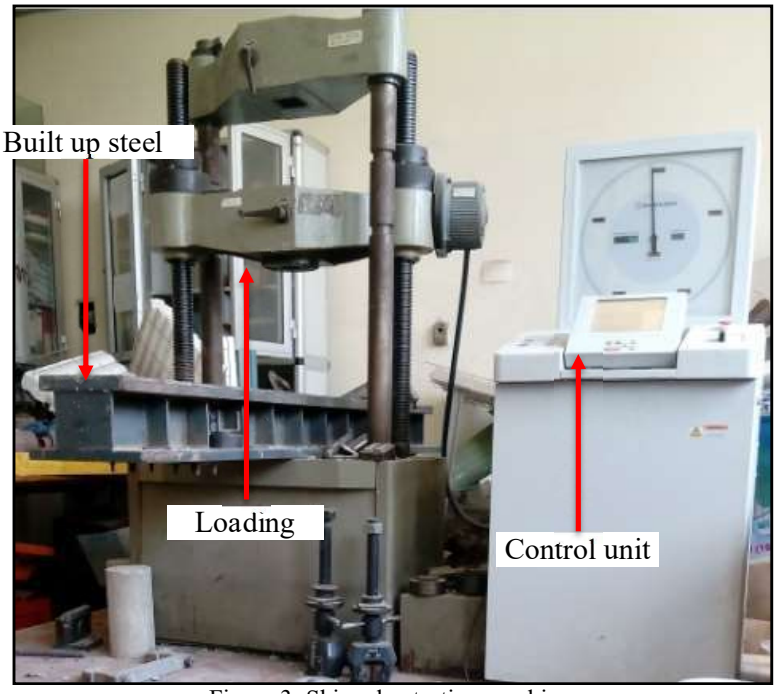

Figure 3: Shimadzu testing machine.

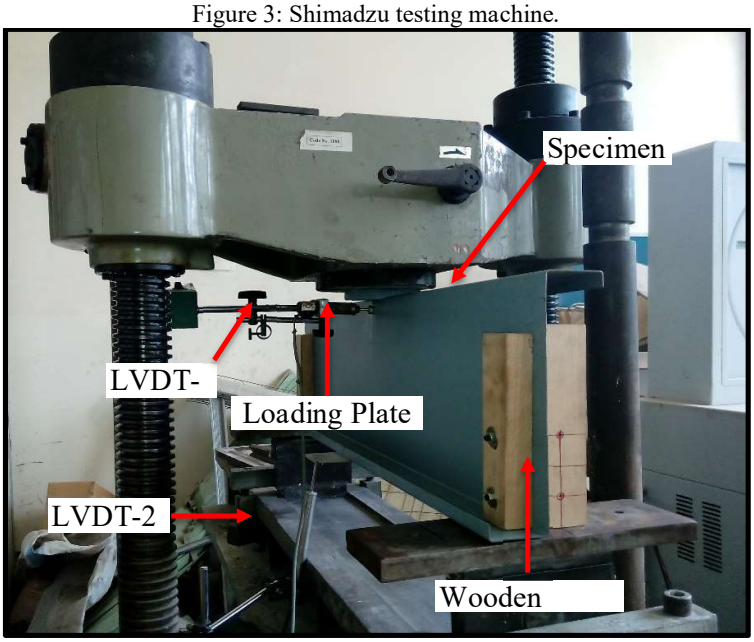

Figure 4 Test rig for IOF loading.

Figure 5 TDS-530 Data logger.

3. Finite Element analysis

The common analysis program ANSYS 14.5 [24] was used to develop nonlinear finite element models. The models were used to simulate the web crippling behavior of the test specimens. The material and geometrical nonlinearities were considered in the finite element models. The models were verified against the experimental test results through the predicted web crippling load P_{FE}, mode of failure and recorded load displacement curves. Extended parametric study was carried out using the verified finite element models to investigate the influence of changing cross section geometries, yield stress and load bearing length on the predicted web crippling strength under IOF loading conditions.

3.1 Modeling

The test specimens were represented in the finite element models by Shell elements of type "shell 181". This shell element is defined by four nodes, each node is defined by six degrees of freedom. Three translations ux, uy and uz and three rotations rox, roy and roz [24]. This type of shell elements suitable for representing plasticity and large strain capabilities. The modeling of test specimens was based on centerline measurements of cross section geometries. A mesh sensitivity study was developed to select the suitable size for shell elements in the developed models. The meshing size was varied along the specimen length as illustrated in Figure 6. A fine meshing of size 2.5×2.5 mm was set for the web area under the load bearing length at mid span. The curved corners were divided into four segments along cross section. A coarse meshing of size 5×5 mm was set for webs, flanges and lips along end bearing locations (100 mm). A meshing sizes of 5×2.5 or 2.5×5 mm were set along the remaining parts of modeled specimen. To account for the material nonlinearity, the stress-strain model developed by Abdel-Rahman and Sivakumaran [25] and shown in Figure 7 was employed. The material properties from tensile tests in table 2 were used to define the stress-strain values according to the adopted model with a Young's modulus of 210 kN/mm^2.

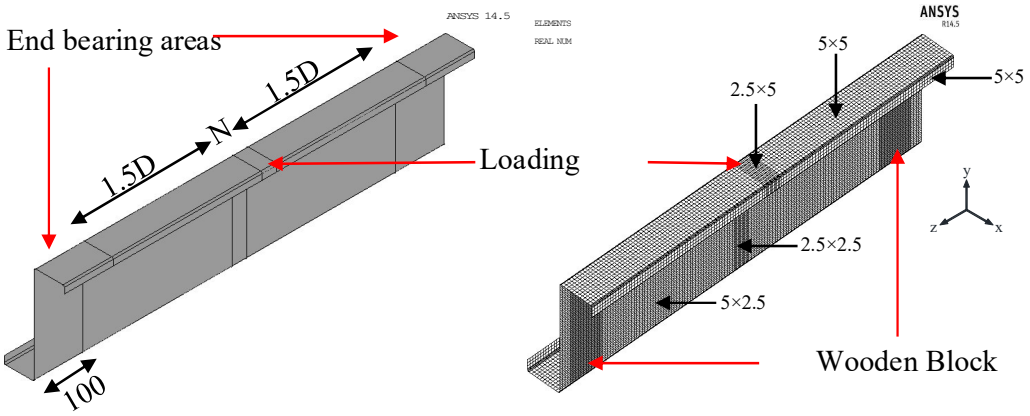

Figure 6: Meshing size along the modeled specimen

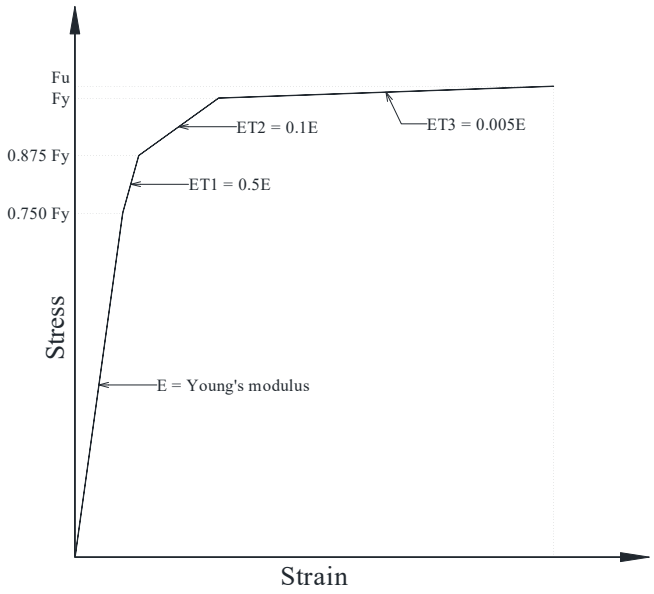

Figure 7: Stress strain model [25].

3.2 Boundary conditions and loading

In the experimental tests, the loading was applied to the specimens through the placed bearing plates on the top flange at the mid span of test specimen. This mid span bearing plate was initially set to be in full contact with the top flange width. But once the loading process starts and the mid span bearing plate became in full contact with the loading jaw, the underlying flange rotates downward about its edge of intersection with the rounded corner connected it to the web and the full contact with the bearing plate is dismissed. Due to this situation and as adopted in [20, 26] the applied load was simulated in the finite element models as nodal loads acting downward at the top edge of the flange-web intersection corner with lateral movement restrained.

To simulate the boundary conditions for the hinge support, the lateral, vertical and longitudinal movements (ux, uy and uz) of the bottom flange were restrained along the center line of the end bearing plate width. To simulate the roller support, only the lateral and vertical movements (ux and uy) of the bottom flange were restrained. Figure 8 shows the pre-described loading and boundary conditions that employed in the model.

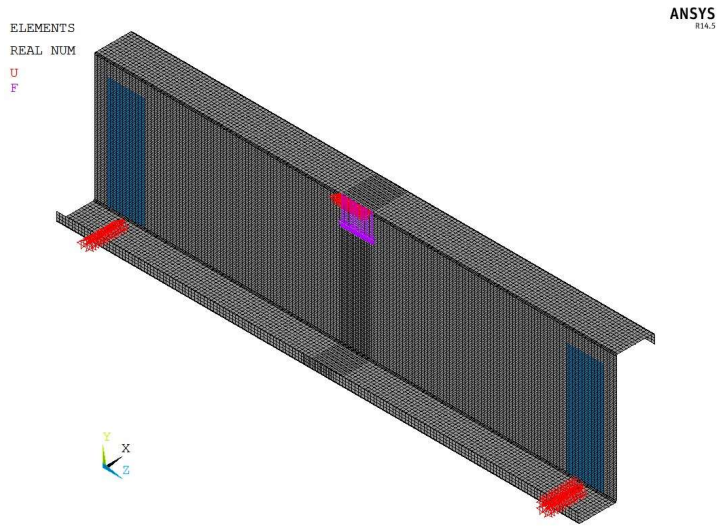

Figure 8: Applied loading and boundary conditions

4. Results and Discussion

In this section, the experimental tests results and finite element analysis were compared in the form of predicted web crippling load, mode of failure and load displacement curves. Furthermore, the results of the extended parametric study were discussed.

4.1 Comparison between experimental tests and finite element analysis

The measured web crippling loads from the experimental tests P_t and the predicted web crippling loads from finite element analysis P_{FE} were listed in Table 3 and compared in terms of load ratios (P_{FE}/P_t). The mean value of load ratios (P_{FE}/P_t), the coefficient of variation COV were 1.0 and 0.02 respectively. The finite element analysis results agreed well with the experimental test results when compared.

Table 3: Experimental tests and finite element web crippling loads

Specimen No.	Specimen Label	P_t, kN	P_{FE}, kN	$\frac{P_{FE}}{P_t}$
S1	Z150×62×16×1.5-R2-N30	6.92	6.96	1.01
S2	Z202×60×00×0.90-R2-N30	1.91	2.39	1.25
S3	Z204×62×16×1.4-R2-N30	6.65	5.98	0.90
S4	Z204×64×16×1.9-R2-N30	12.51	13.71	1.10
S5	Z204×62×00×1.5-R2-N30	6.84	6.73	0.98
S6	Z204×62×16×1.4-R2-N50	7.78	6.75	0.87
S7	Z204×60×00×1.5-R2-N50	7.98	7.92	0.99
S8	Z204×62×16×1.4-R2-N100	9.60	9.50	0.99
S9	Z202×62×00×1.4-R2-N100	8.37	8.29	0.99
S10	Z254×62×16×1.5-R2-N30	7.85	6.84	0.87
S11	Z202×62×16×1.1-R2-N30	3.08	3.62	1.18
S12	Z203×62×16×1.0-R2-N100	4.35	5.27	1.21
Avg				1.03

COV		0.02

4.2 General behavior and failure mode

The load displacement curves *P-ux* and *P-uy* of specimen S1 from experimental test and finite element analysis were plotted in Figure 9. The load displacement relationships showed initially linear elastic behavior up till load value 6.4 kN. After that, the relationships showed inelastic behavior up till the web crippling at load value 6.9 kN. Beyond this load the relationship showed plastic behavior up till failure. The initial linear elastic behavior represented the rotation of the top flange down ward around the top edge of flange web rounded corner, losing the full contact with the load bearing plate. The inelastic behavior represented the transfer of the applied load along the bearing plate length through the top rounded corner to the web up till web crippling occurs. The plastic behavior represented the formation of plastic hinges in web under the load bearing plate.

The load displacement curves *P-ux* and *P-uy* and the failure modes obtained from the experimental tests and finite element analysis showed a good agreement, Figures 9 and 10. The comparisons between load displacement relationships *P-ux* and *P-uy* in figure 9 showed that the local web deformation under loading significantly controlled the global deformation of the specimen and caused its failure due to web crippling. This was noted for all the tested specimens.

The induced stresses in the material surrounding the crippled web area at the bottom flange was elastic up to failure as shown in the finite element results. The Von Mises and y-y stresses at web crippling were presented in figure 11. The crippled part of the web behaved as a quadrilateral plate subjected to axial eccentric load and supported along its sides by springs having different rotational stiffness. The web crippling occurred at yielding of the crippled web cross section.

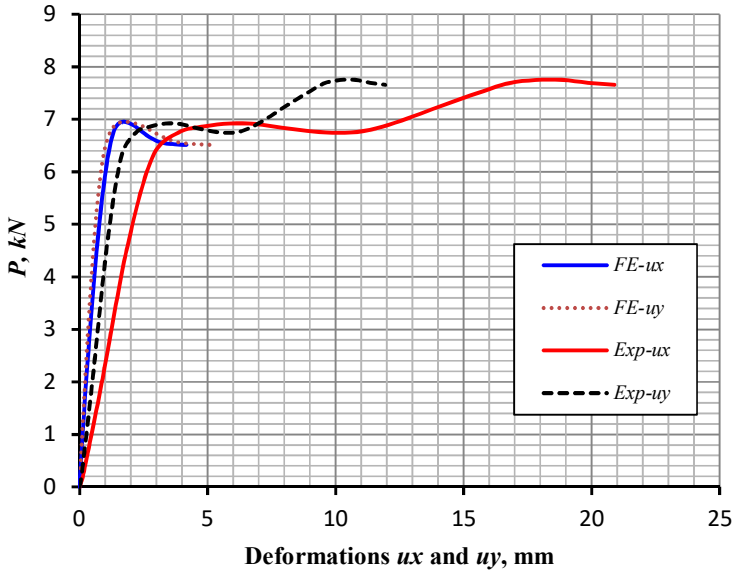

Figure 9: Relationships of *P- ux* and *P-uy* of specimen S1.

a) Experimental test.

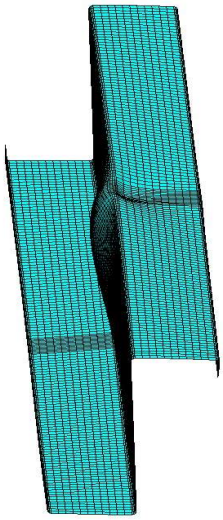

(b) Finite element analysis.

Figure 10: Specimen failure modes of S1.

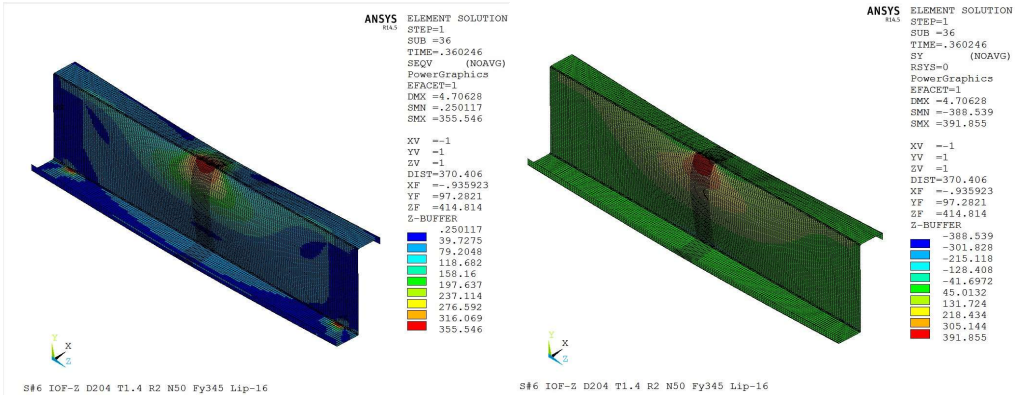

(a) Specimen-S6.

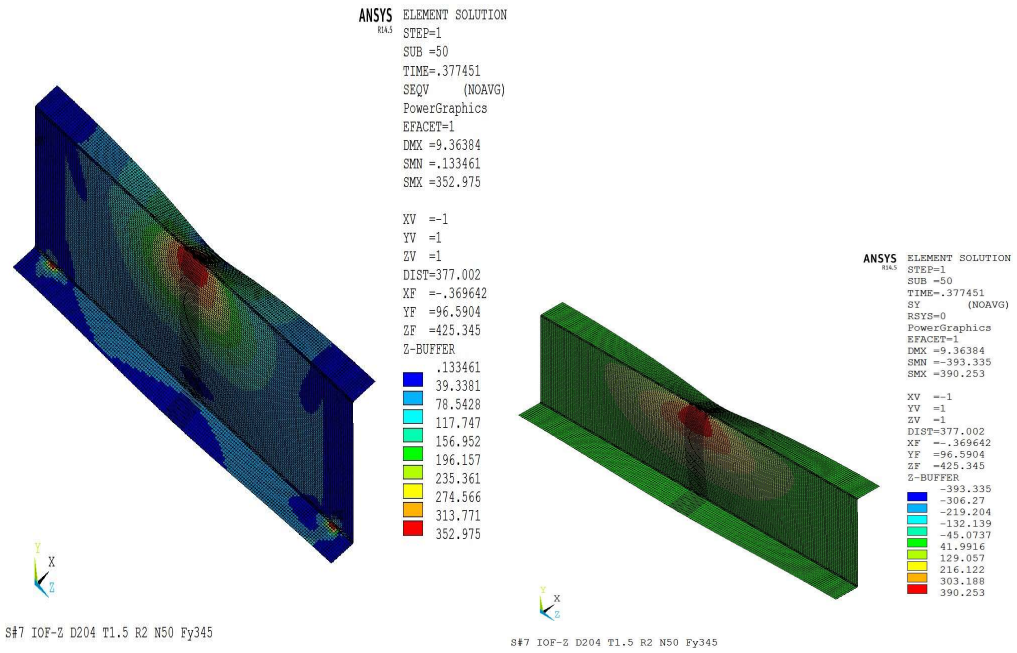

(b) Specimen- S7.

Figure 11: Von Mises and y-y stresses of S6 and S7

4.3 Effect of cross section geometries on web crippling

The verified finite element models were employed to study the variation of web crippling loads P_{FE} due to changing the defined dimensions of Z section. Specimens with similar cross section dimensions, except for the considered variable were used. The material properties for this study were; yield stress (F_y =345 N/mm^2), ultimate stress (F_u =415 N/mm^2) and Young's modulus (E =*210 kN/mm*^{2}). Hereafter, the obtained results from the finite element analysis and the experimental tests used for explaining the results.

4.3.1 Effect of web thickness *t*

The variation of the web crippling loads P_{FE} web thickness t at different values of load bearing length N were presented in figure 12. It was observed that, changing the web thickness has a very significant effect on the web crippling loads which are in direct proportional to the web thickness t. Increasing the web thickness from 1 mm to 2 mm, caused an increase in the web crippling load by 300% and 290% at bearing length N = 75 and 150 mm respectively. Increasing the web thickness to 3 mm, caused an increase in the web crippling load by 760 and 740% at bearing length N = 75 and 150 mm respectively. Comparing the experimental test results from specimens; S3, S4 and S11 of nearly the same dimensions except the web thickness showed the same effect, Figure13. However, the yield stress of specimen S4 was 33% larger than S11, Increasing the web thickness from 1.1 mm in S11 to 1.90 mm in S4 caused significant increase in the crippling load by 306%. The comparison between specimens S12 and S8 from Table 3, where the web thickness increased by 40% and F_y increased by 15%, resulted in increasing the web crippling load by 121%. For the specimens with no lip, the comparison between S2 and S5 showed the same conclusion. Increasing the web thickness t has two opposite effects.

The first effect is increasing the eccentricity of the applied load and so magnifying the induced moment on the crippled web plate. On the other side, the second effect is increasing the cross sectional area and the moment of inertia of the crippled web plate, hence reducing the induced stresses. Furthermore, the web thickness proportional to the stiffness of the surrounding parts to the crippled web area and the flanges. The second effect is significantly more effective than the first one and so the increase in the web crippling load was significant. This was noted when comparing the load displacement curves of S11, S3 and S4 at the elastic stage, Figure 13. Specimen S4 showed stiffer behavior than S11 and S3.

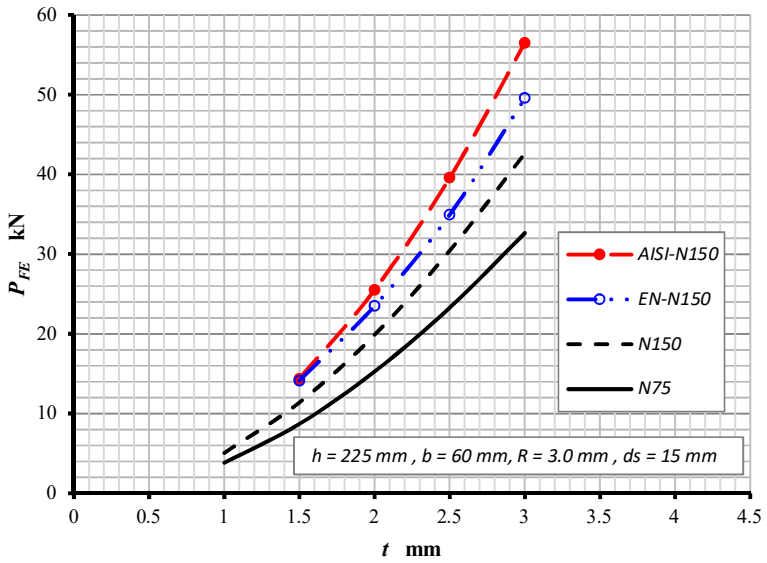

Figure 12 Variation of web crippling P_{FE} with web thickness t at different N values.

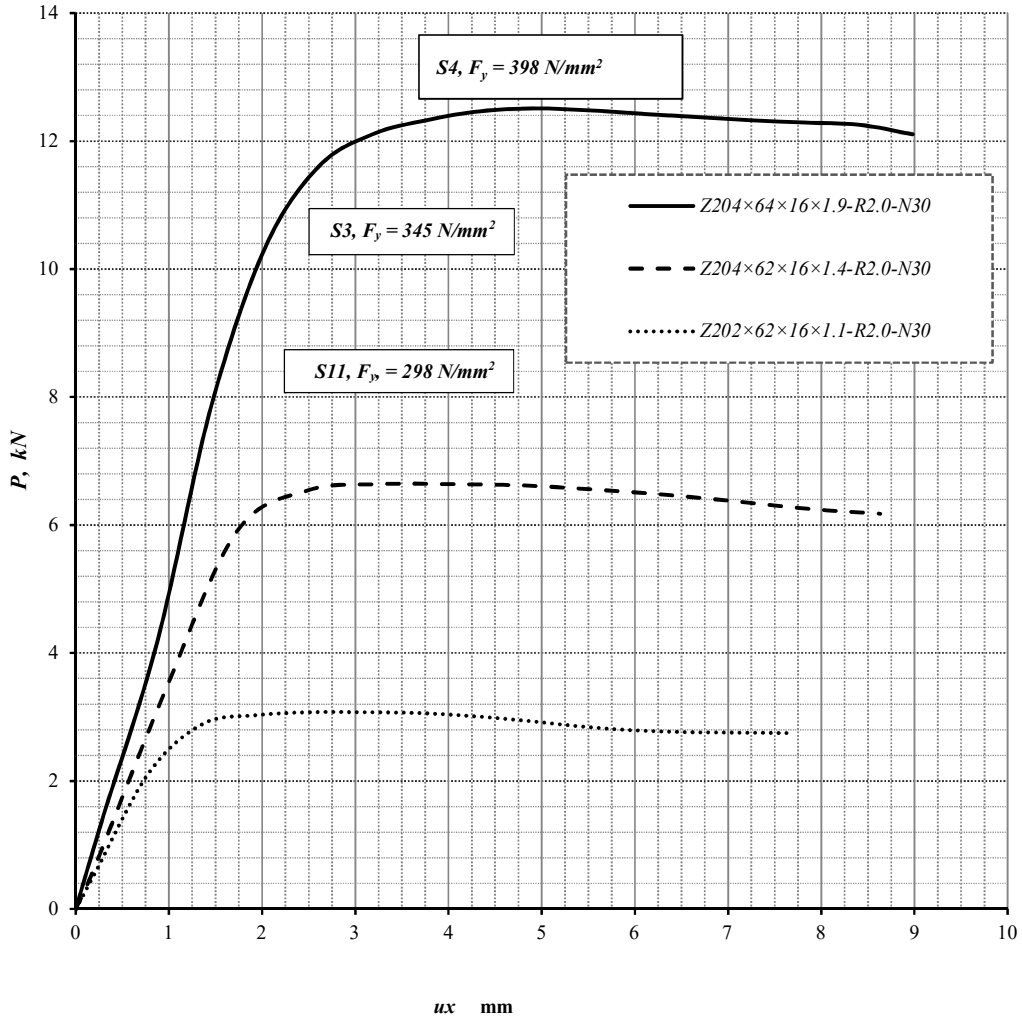

Figure 13: load displacement curves of specimens S3, S4 and S11.

4.3.2 Effect of web height *h*

The web crippling loads P_{FE} are inversely proportional to the flat web height *h*, Figure 14. The value of *N* magnified this effect. The increase of flat web height *h* from 150 mm to 225 mm, i.e. 50%, caused reductions in P_{FE} values by 3.5% and 8.5% at *N*= 75 and 150 mm respectively. The increase of *h* to 375 mm, i.e. 150%, caused reduction in P_{FE} values by 9% and 19% at *N*= 75 and 150 mm respectively. The values of flat web height *h* and web thickness *t* of specimen S3 were 38% more and 10% less respectively than those of S1. This caused a reductions in the web crippling load P_t of S3 by 4% compared to S1. The increase of *h* in S10 compared to S1, caused an increase in web crippling load by 13%. This was different to the finite element findings and explained as follows. Exploring figure 14 at *N*=75 mm, the increase of *h* from 150 to 254 mm as in the case of S1 and S10 caused a reduction in web crippling load P_{FE} by 4%. The reduction in P_t value was expected to be even less in the case of S10 in comparison to S1 because *N*= 30 mm. The low (P_{FE}/P_t) ratio of S10 concealed the effect of *h*, table 3. The increase of *h* has two opposite effects. The effected width of the web plate part, at the maximum lateral web deformation occurs assuming 45° load distribution, would increase. Both the cross sectional area and the moment of inertia of that effected part of the web plate increased and the induced axial and bending stresses reduced. On the contrary, the increase of *h* increased the span between the top and bottom flanges that providing rotational support to the web plate. This reduced the flexural stiffness of the web plate promoting crippling.

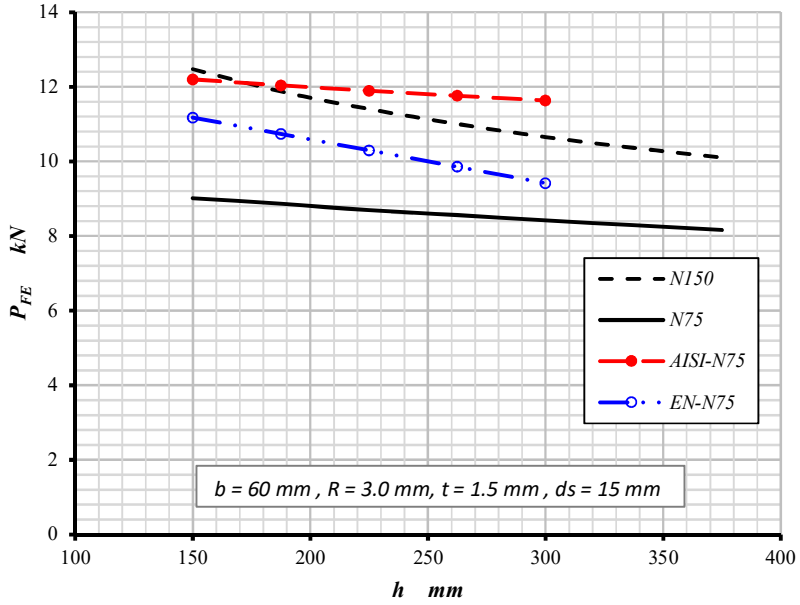

Figure 14. Variation of P_{FE} and *h* at different *N* values.

4.3.3 Effect of inside bent radius *R*

The web crippling loads P_{FE} are inversely proportional to the inside bent radius *R* and the increase of the load bearing length N minimizes this effect, Figure 15. The increase of *R* from 1 mm to 3 mm, i.e. by 200%, caused reductions in P_{FE} values by 28% and 21% at *N*= 75 and 150 mm respectively. The increase of *R* to 7.5mm, i.e. 650%, caused 52% and 43% reductions in P_{FE} values at *N*= 75 and 150 mm respectively. Increasing the value of *R* increased the eccentricity of the applied load, the induced moment and the lateral deformation of the web plate promoting crippling.

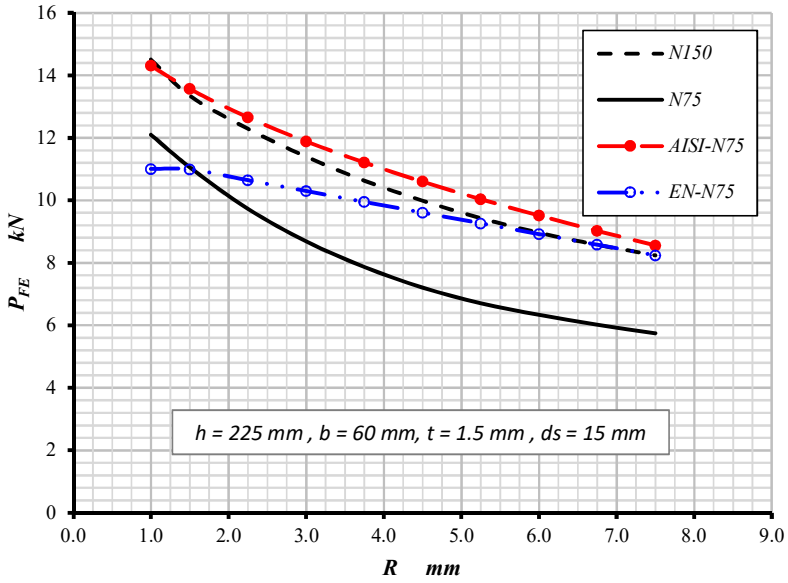

Figure 15: Variation of P_{FE} and R at different N values.

4.3.4 Effect of lip depth *ds*

The web crippling loads P_{FE} are proportional to the lip depth *ds* as shown in Figure 16. By using lip of depth equal to 25%, 50% and 100% of *b* at *N*=75 mm, the value of P_{FE} increased by 12%, 18% and 21% respectively in comparison to un-stiffened cross section where ds=0. The increase of *N* to 150 mm has magnified the effect of *ds* and the values of P_{FE} have increased by 15% and 37% respectively. The comparison between the web crippling load of specimens S8 and S9 in Table3 shoed nearly the same results. The use of lip having depth of 25% of *b* in S8 increased the web crippling load P_t by 15% in comparison to that of S9. The use of the lip stiffened the behavior of S8 as shown in Figure 19. The further comparison of S3 and S6 results to those of S5 and S7 may lead to inaccurate conclusions because the dimensions of the different details of the counterpart specimens, lipped and un-lipped, are not typical.

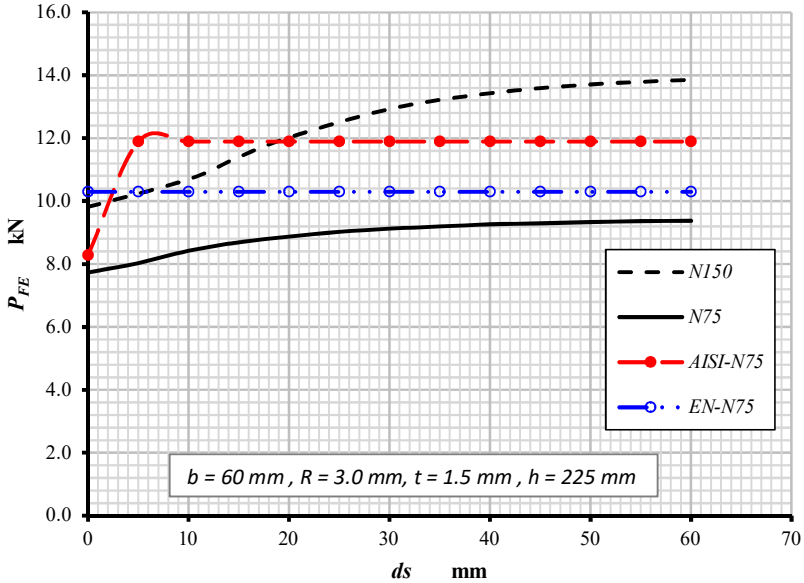

Figure 16: Variation of P_{FE} and *ds* at different *N* values.

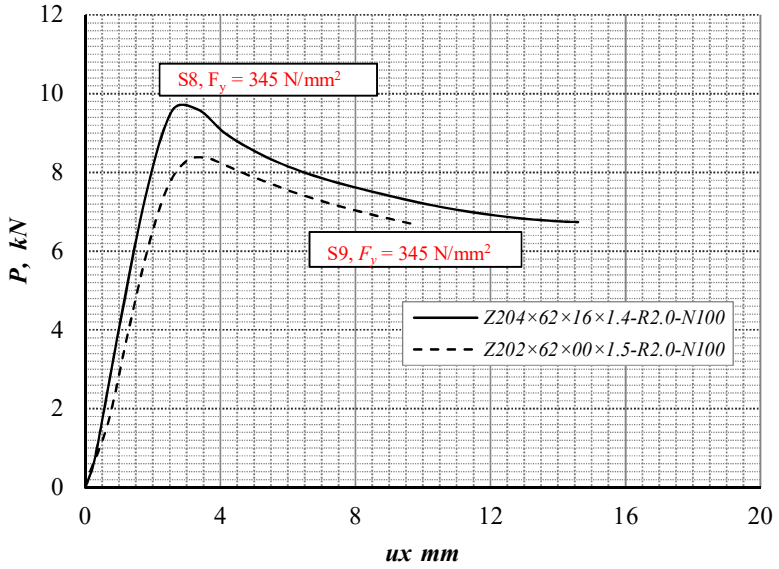

Figure 17 Load displacement curves of specimens S8 and S9.

4.3.5 Effect of Load bearing length *N*

The specimens considered in this section have typical dimensions and different *N* values. The values of web crippling load P_{FE} are proportional to the load bearing length *N*, Figure 18. Comparing the web crippling load values P_t of the stiffened specimens S3, S6 and S8 and of the un-stiffened specimens S5, S7 and S9 showed the same effect. The load displacement curves of test specimens S3, S6 and S8 and those of S5, S7 and S9 were plotted in figures 19 and 20 respectively. The increase of load bearing length *N* increased the width of the affected area of the web plate at which the load distributed. This increased length reduced the induced axial load and moment per unite length of the effected web plate cross section, the lateral deformation *ux* and hence increasing the web crippling load.

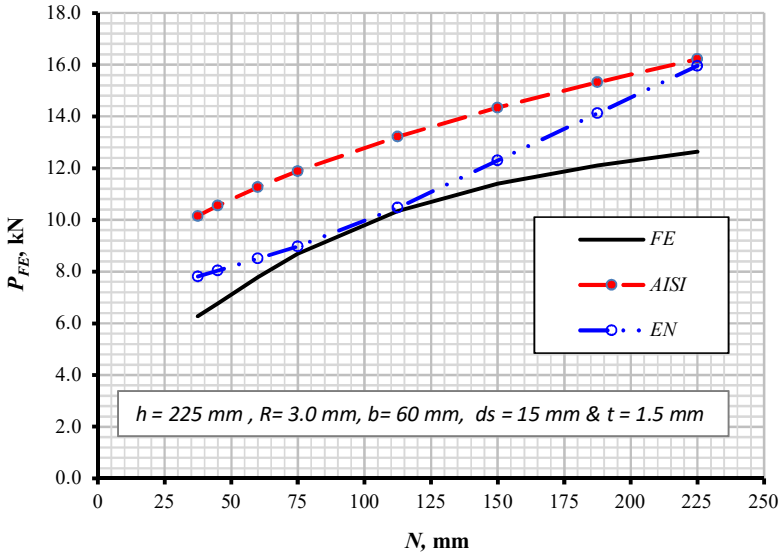

Figure 18 Variation of web crippling load P_{FE} and load bearing length *N*.

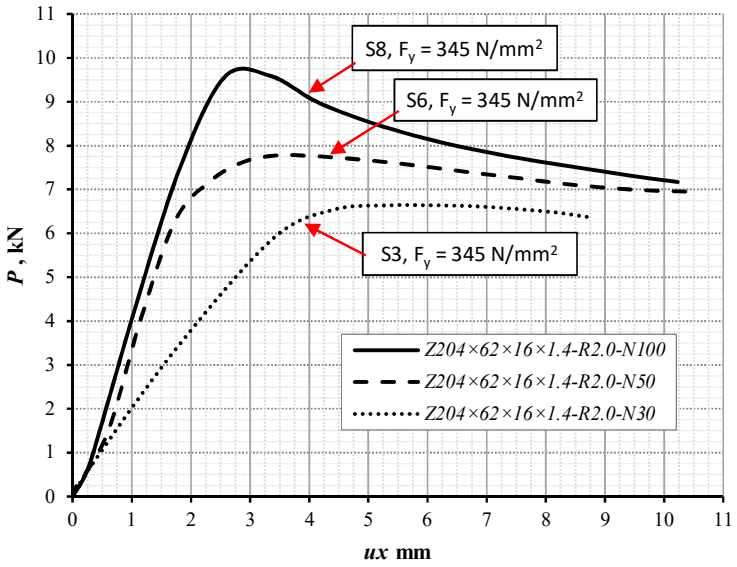

Figure 19 Load displacement curves of test specimens S3, S6 and S8.

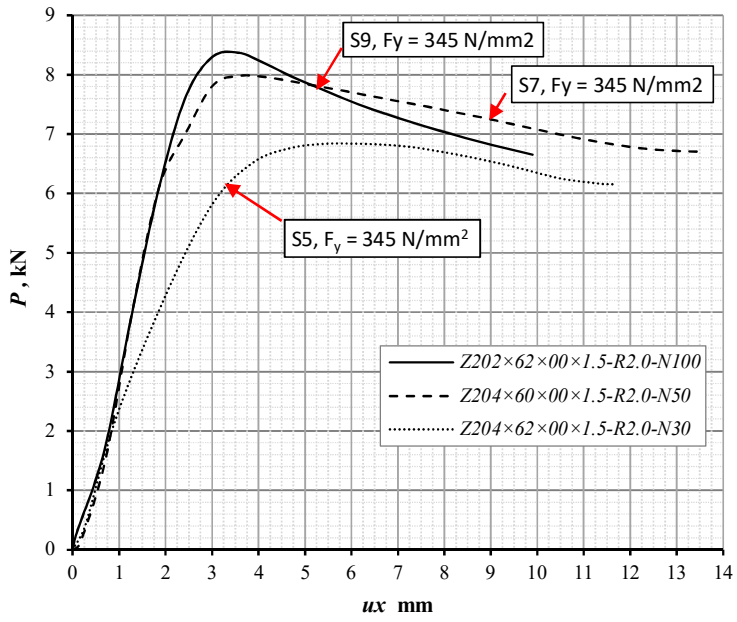

Figure 20 Load displacement curves of test specimens S5, S7and S9.

5. Codes of practice

In this section, the design expressions from the American specification AISI S100-16 [22] and the Eurocode EN 1993-3-1 [15] were calibrated against the obtained results in this study and the results of reference [27] for members of Z section subjected to IOF loading condition.

5.1 Design expressions

The following expressions were provided in the AISI S100-16 [22] for calculating the nominal web crippling strength $P_{n\text{-}AISI}$ of cold formed steel section Z sections provided that, $h/t \leq 200$, $N/t \leq 210$, $N/h \leq 2.0$ and $\theta = 90°$;

$$P_{n-AI} = C.t^2.F_y.Sin\,\theta\left(1 - C_R\sqrt{\frac{R}{t}}\right).\left(1 + C_N\sqrt{\frac{N}{t}}\right).\left(1 - C_h\sqrt{\frac{h}{t}}\right) \quad (1)$$

The coefficients C, C_R, C_N and C_h are listed in Table 4 for single web Z-sections having flanges un-fastened to supports and subjected to web crippling under IOF loading condition. The other symbols in the formula are as defined before.

Table 4: Web crippling coefficients for Z sections subjected to IOF loading

Support conditions	Stiffened flanges				Un-Stiffened flanges			
	C	C_R	C_N	C_h	C	C_R	C_N	C_h
Un-fastened to support	13.0	0.23	0.14	0.01	13.0	0.32	0.10	0.01

In the Eurocode EN 1993-1-3 [15], the web transverse resistance for cross-sections having single un-stiffened web and subjected to IOF loading, is calculated according to the following expressions, provided that, $h/t \leq 200$, $R/t \leq 6$ and $45° \leq \theta \leq 90°$;

$$P_{n-EN} = k_3.k_4.k_5\,t^2.F_y\left(14.7 - \frac{h_w/t}{49.5}\right).\left(1 + 0.007\frac{N}{t}\right)/\gamma_{M1} \qquad For\ N/t \leq 60 \quad (2)$$

$$P_{n-EN} = k_3.k_4.k_5\,t^2.F_y\left(14.7 - \frac{h_w/t}{49.5}\right).\left(0.75 + 0.011\frac{N}{t}\right)/\gamma_{M1} \qquad For\ N/t > 60 \quad (3)$$

Where;

$k = F_y/228$

$k_3 = 0.7 - 0.3\,(\theta/90)^2$

$k_4 = 1.22 - 0.22\,k$

$k_5 = 1.06 - 0.06\,R/t \qquad k_5 \leq 1.0$

$\gamma_{M1} = 1.00$

5.2 Comparison of the web crippling loads and strengths

The web crippling strengths ($P_{n\text{-}AISI}$ and $P_{n\text{-}EN}$) according to the design expressions 1, 2 and 3 were calculated for the cases considered in this study provided that satisfying the design limits. The web crippling strengths ($P_{n\text{-}AISI}$ and $P_{n\text{-}EN}$) were plotted previously in figures 12, 14, 15, 16 and 18. In general, it was observed that the design specifications AISI S100-16 [22] and EN 1993-1-3 [15] overestimated the web crippling strengths compared to the predicted web crippling loads P_{FE} obtained from finite element analysis. The web crippling strengths $P_{n\text{-}AISI}$ and $P_{n\text{-}EN}$ were found proportional to the web thickness t and the load bearing length N and inversely proportional to h and R. This agrees with both the experimental and finite element findings. As shown in figures 12,14,15,16 and 18, the relationships between $P_{n\text{-}AISI}$ and the different cross section dimensions and bearing lengths were nearly similar in pattern to those obtained using the finite element analysis.

This was not the same for the relationships of $P_{n\text{-}EN}$. However, the resistance factors were excluded from all the design expressions, the two design codes produced different values of the web crippling strength for the same cases. The overestimation in the web crippling strength due to the design specification AISI 100-16 [22] was more than the design standard EN 1993-1-3 [15]. The effects of the lip depth ds was not considered in the specs. For more accurate comparison, the web crippling test loads from the experimental study in reference [27] in addition to the experimental test loads P_t and predicted web crippling loads P_{FE} from finite element analysis in this study were plotted against $P_{n\text{-}AISI}$ and $P_{n\text{-}EN}$ in Figures 21 and 22 respectively. The considered design expressions overestimated the web crippling strength in most of the considered cases. The average, minimum and maximum values of the ratios $P/P_{n\text{-}AISI}$ and $P/P_{n\text{-}EN}$ were listed in Table 5 where P is the web crippling load either obtained from experimental tests or using the finite element analysis.

Table 5 Comparisons between web crippling load ratios P/P_n

Design Specification	P/P_n	Min	Max	Avg	COV
AISI S100-16 [22]	$P/P_{n\text{-}AISI}$	0.62	1.01	0.77	0.008
EN 1993-1-3[15]	$P/P_{n\text{-}EN}$	0.70	1.10	0.84	0.007

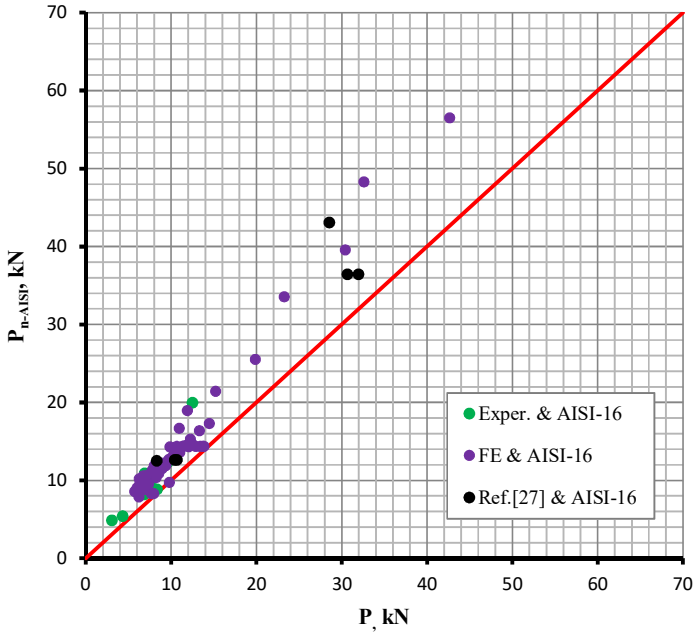

Figure 21: Comparison of $P_{n\text{-}AISI}$ and P values.

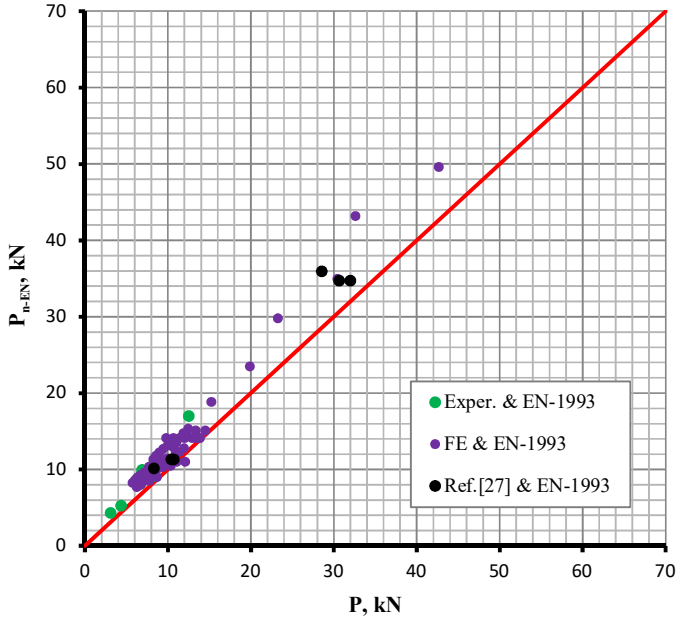

Figure 22: Comparison of $P_{n\text{-}EN}$ and P values.

6. Conclusion

In this research, the test program was designed to study the influence of changing the cross section dimensions on the web crippling strength of cold formed steel Z sections subjected to interior one flange IOF loading condition. The tools used in this study were; the experimental tests, the finite element analysis and the design specifications. The results obtained from the experimental test carried out in this research and from reference [27] in addition to the results of the verified finite element analysis were compared to the code design approaches. Based on the results of different comparisons, the following points were concluded;

The developed finite element models using ANSYS software are a very good tool for simulating the web crippling behavior of tests. The average difference between the developed finite element analysis and the experimental test results is 3%, with a variance of 0.02. This means that, the developed finite element model is a reliable tool to predict the web crippling strength of Z-sections.

The design expressions considered in this study are not conservative for predicting the web crippling nominal strengths compared to both finite element and experimental test results. Further adjustments are recommended to be applied for the studied design approaches.

Based on the results of web crippling strength and load variations with cross section dimensions, the web thickness among all cross section geometries is considered of the major effect on web crippling strength. The web thickness t is directly proportional to the web crippling strength. On contrary, the inside bent radius R and/or flat web height are inversely proportional to the web crippling strength. The effect of the inside bent radius on decreasing the web crippling strength is more significant than the flat web height effect.

Two cross section dimensions were not considered in the design expressions; the flange width b and lip depth ds. In this study the effect of the lip depth is considered and it was found effective to some extent at least the web crippling strength increased by 12% when the lip depth to flange width was (ds/b = 0.25). Further study is recommended to study the influence of flange width on the web crippling strength.

Finally, the load bearing length N is also directly proportional to the web crippling strength and the relationship is nearly linear.

References

1- B. H. Bhakta, R. A. LaBoube, W. W. Yu, “The Effect of Flange Restraint on Web Crippling Strength”, Final Report, Civil Engineering Study 92-1, University of Missouri-Rolla, Rolla, Missouri, U.S.A., March 1992.

2- D. E. Cain, R. A. LaBoube, W. W. Yu, “The Effect of Flange Restraint on Web Crippling Strength of Cold Formed Steel Z-and I-Sections”, Final Report, Civil Engineering Study 95-2, University of Missouri-Rolla, Rolla, Missouri, U.S.A., May 1995.

3- AISI 1986-American Iron and Steel Institute, "Cold-Formed Steel Design Manual: Specification for the Design of Cold-Formed Steel Structural Members," August 19, 1986, with December 11, 1989 Addendum.

4- R. R. Gerges, R. M. Schuster, "Web Crippling of Single Web Cold Formed Steel Members Subjected to End One-Flange Loading", Fourth International Specialty Conference on Cold-Formed Steel Structures, St. Louis, Missouri, U.S.A., October, 1998

5- AISI 1996 – Specification for the Design of Cold-Formed Steel Structural Members, American Iron and Steel Institute, 1996 Edition, Washington DC.

6- CSA S136-94 – Cold Formed Steel Structural Members, Canadian Standards Association, Rexdale (Toronto), Canada, December 1994.

7- B. Beshara, R. M. Schuster, "Web Crippling Data and Calibrations of Cold Formed Steel Members", Research Report RP00-2, Canadian Cold Formed Steel Research Group, University of Waterloo (AISI Report, Revised 2006), Canada, (2000).

8- NAS 2001 "North American Specification for the design of cold-formed steel structural members". Washington, DC: American Iron and Steel Institute; 2001.

9- B. Young, G. J. Hancock, "Design Of Cold-Formed Channels Subjected To Web Crippling", Journal of Structural Engineering, Vol. 127, No. 10, October, 2001.

10- B. Young, G. J. Hancock, "Cold-Formed Steel Channels Subjected to Concentrated Bearing Load", Journal of Structural Engineering, Vol. 129, No. 8, August 1, 2003.

11- B. Young, G. J. Hancock, "Web crippling of cold-formed unlipped channels with flanges restrained", Thin-Walled Structures 42 (2004) 911–930.

12- M. W. Holesapple, R. A. LaBoube, "Web crippling of cold-formed steel beams at end supports", Engineering Structures 25 (2003) 1211–1216.

13- M. Macdonald, M.A. Heiyantuduwa, M. Kotelko, J. Rhodes, "Web crippling behaviour of thin-walled lipped channel beams", Thin-Walled Structures 49 (2011) 682–690.

14- M. Macdonald, M.A. Heiyantuduwa, "A design rule for web crippling of cold-formed steel lipped channel beams based on nonlinear FEA", Thin-Walled Structures 53 (2012) 123–130.

15- EN 1993-1-3:2006, CEN European Committee for Standardization, Euro code 3: Design of steel structures Part 1-3: General rules - Supplementary rules for cold formed members and sheeting, CEN, Brussels, Belgium, 2006.

16- S. Gunalan, M. Mahendran, "Web crippling tests of cold-formed steel channels under two flange load cases", Journal of Constructional Steel Research 110 (2015) 1–15.

17- AS/NZS 4600. Cold-formed steel structures. Australian/New Zealand Standard. Sydney, Australia: Standards Australia; 2005.

18- AISI S100-2007. North American Specification for the Design of Cold-Formed Steel Structural Members, American Iron and Steel Institute (AISI), Washington, DC, U.S.A.

19- L. Sundararajah, M. Mahendran, P. Keerthan, "New design rules for lipped channel beams subject to web crippling under two-flange load cases", Thin-Walled Structures 119 (2017) 421–437.

20- L. Sundararajah, M. Mahendran, P. Keerthan, "Web crippling experiments of high strength lipped channel beams under one-flange loading", Journal of Constructional Steel Research 138 (2017) 851–866.

21- AISI S100-2012. American Iron and Steel Institute (AISI), Specifications for the cold-formed steel structural members, cold-formed steel design manual, AISI S100, Washington DC, USA, 2012.

22- AISI S100-16. North American Specification for the Design of Cold-Formed Steel Structural Members, American Iron and Steel Institute (AISI), Washington, DC, U.S.A, 2016.

23- ASTM A370 (2016). Standard Method and Definitions for Mechanical Testing of Steel Products.

24- ANSYS 14.5, User's Manual. Swanson Analysis System, U.S.A., 2012.

25- N. Abdel-Rahman and K. S. Sivakumaran, "Evaluation and Modeling of the Material Properties for Analysis of Cold-formed Steel Sections", International Specialty Conference on Cold-Formed Steel Structures, October 17, 1996.

26- A. P. C. Duarte, N. Silvestre, "A New Slenderness-based Approach for the Web Crippling Design of Plain Channel Steel Beams", International Journal of Steel Structures September 2013, Vol 13, No 3, 421-434.

27- M. W. Holesapple, R. A. LaBoube, "Overhang Effects on End-One-Flange Web Crippling Capacity of Cold-Formed Steel Members." Final Report, Civil Engineering Study 02-1, May 2002, University of Missouri – Rolla.